Phosphoenolpyruvate carboxykinase (*Pck1*) helps regulate the triglyceride/fatty acid cycle and development of insulin resistance in mice[S]

Carrie A. Millward,* David DeSantis,* Chang-Wen Hsieh,* Jason D. Heaney,[†] Sorana Pisano,* Yael Olswang,[§] Lea Reshef,[§] Michelle Beidelschies,* Michelle Puchowicz,* and Colleen M. Croniger[1,*]

Departments of Nutrition* and Genetics,[†] Case Western Reserve University, Cleveland, OH 44106; and Department of Developmental Biochemistry,[§] Hebrew University-Hadassah Medical School, Jerusalem 91120, Israel

Abstract The aim of this study was to investigate the role of the cytosolic form of phosphoenolpyruvate carboxykinase (*Pck1*) in the development of insulin resistance. Previous studies have shown that the roles of *Pck1* in white adipose tissue (WAT) in glyceroneogenesis and reesterification of free fatty acids (FFA) to generate triglyceride are vital for the prevention of diabetes. We hypothesized that insulin resistance develops when dysregulation of *Pck1* occurs in the triglyceride/fatty acid cycle, which regulates lipid synthesis and transport between adipose tissue and the liver. We examined this by analyzing mice with a deletion of the PPARγ binding site in the promoter of *Pck1* (PPARE$^{-/-}$). This mutation reduced the fasting *Pck1* mRNA expression in WAT in brown adipose tissue (BAT). To analyze insulin resistance, we performed hyperinsulinemic-euglycemic glucose clamp analyses. PPARE$^{-/-}$ mice were profoundly insulin resistant and had more FFA and glycerol released during the hyperinsulinemic-euglycemic clamp compared with wild-type mice (WT). Finally, we analyzed insulin secretion in isolated islets. We found a 2-fold increase in insulin secretion in the PPARE$^{-/-}$ mice at 16.7 mM glucose. Thus, the PPARE site in the *Pck1* promoter is essential for maintenance of lipid metabolism and glucose homeostasis and disease prevention.—Millward, C. A., D. DeSantis, C-W. Hsieh, J. D. Heaney, S. Pisano, Y. Olswang, L. Reshef, M. Beidelschies, M. Puchowicz, and C. M. Croniger. **Phosphoenolpyruvate carboxykinase (*Pck1*) helps regulate the triglyceride/fatty acid cycle and development of insulin resistance in mice. *J. Lipid Res.* 2010.** 51: **1452–1463.**

Supplementary key words adipocytes • adipose tissue • diabetes • glucose • triglycerides

Obesity and type 2 diabetes are growing epidemics worldwide in adults and children. The incidence of type 2 diabetes increased by 10-fold from 1982 to 1994 and is expected to reach 366 million worldwide in 2030 (1, 2). Therefore, it is important to determine the causes of this disease and develop preventive strategies as well as more effective treatments. One risk factor for the development of type 2 diabetes is elevated free fatty acids (FFA) in the blood. Elevated FFAs have been shown to induce insulin resistance in peripheral tissues by inhibiting insulin-stimulated glucose uptake and glycogen synthesis (3–5).

In the fed state, triglycerides are synthesized using glycerol-3-phosphate generated from the oxidation of glucose. In the fasted state, however, insulin levels are lower and lipolysis occurs. A significant amount of FFA is reesterified to generate triglyceride in the fasted state in white adipose tissue (WAT) and liver. Since glucose is limited in the fasted state, the ability to generate glycerol-3-phosphate from glucose in adipose tissue is greatly reduced. Also, due to negligible levels of glycerol kinase (GyK) expression in adipose tissue, glycerol-3-phosphate cannot be generated from glycerol. Reshef et al. showed that gluconeogenic

This work was supported by the National Institute of Diabetes and Digestive and Kidney Diseases (NIDDK) Grant DK-075040 (C.M.C.) and National Institutes of Health Metabolism Training Grant T32-DK-007319 (C.A.M. and M.B.). The clamp studies performed at the Mouse Metabolic Phenotyping Center of Vanderbilt University (Nashville, TN) were supported by NIDDK Grant U24-DK-59637. The triglyceride synthesis studies performed at the Mouse Metabolic Phenotyping Center of Case Western Reserve University (Cleveland, OH) were supported by NIDDK Grant DK-76769. Metabolic rates measured by indirect calorimetry in WT and PPARE$^{-/-}$ mice at the Mouse Metabolic Phenotyping Center of the University of Cincinnati (Cincinnati, OH) were supported by NIDDK DK59630. Its contents are solely the responsibility of the authors and do not necessarily represent the official views of the National Institutes of Health or other granting agencies.

Manuscript received 11 January 2010 and in revised form 2 February 2010.

Published, JLR Papers in Press, February 2, 2010
DOI 10.1194/jlr.M005363

Abbreviations: BAT, brown adipose tissue; CS, citrate synthase; GIR, glucose infusion rate; GTT, glucose tolerance test; GyK, glycerol kinase; IP, intraperitoneally; Pck1, phosphoenolpyruvate carboxykinase; SDH, succinate dehydrogenase; UCP, uncoupling protein; WAT, white adipose tissue; WT, wild type.

[1] To whom correspondence should be addressed.
e-mail: cmc6@case.edu

[S] The online version of this article (available at http://www.jlr.org) contains supplementary data in the form of one table and two figures.

precursors, such as pyruvate, lactate, and alanine, are converted into the glycerol backbone of triglyceride by *Pck1* and the glyceroneogenic pathway (6) (7, 8).

In brown adipose tissue (BAT), glyceroneogenesis has been shown to generate as much as 81% of total glycerol-3-phosphate in rats. Hahn and Novak suggested that maintenance of triglyceride stores in the BAT is associated with activation of heat production. They proposed that FFA released from triglyceride were substrates for BAT mitochondria and increase the expression of uncoupling proteins (UCP) (9).

Glyceroneogenesis has also been described for the liver during fasting (10, 11). FFA released from adipose tissue is oxidized and converted to ketone bodies and carbon dioxide. However, a significant portion of the FFA (60%) is reesterified back to triglyceride and packaged into VLDL in the liver. VLDL can then be released for transport to muscle and adipose tissues (10, 12) (13). Therefore, the liver plays a central role in the triglyceride/fatty acid cycle, and the pathway of glyceroneogenesis is essential for regulation of the FFA flux in the triglyceride/fatty acid cycle (14).

The aim of this study was to examine the role of *Pck1* in the regulation of the triglyceride/fatty acid cycle in the liver and WAT. To accomplish this, we analyzed PPARE$^{-/-}$ mice (15) that have 0.2% *Pck1* mRNA expression of WT in WAT, 20% *Pck1* mRNA expression of WT in BAT, and altered regulation of *Pck1* mRNA expression in the liver.

METHODS

Generation of PPARE$^{-/-}$ mice

Mice with reduced *Pck1* mRNA expression in WAT were generated as previously described (15). Briefly, E14 embryonic stem (ES) cells (129/OlaHsd) were manipulated to generate male chimeric mice, and these mice were mated with C57BL/6J female mice, resulting in heterozygous offspring. The mice were intercrossed (brother × sister matings) for over 20 generations to make a stable isogenic strain. Mice containing the wild-type promoter sequence were designated wild-type mice (WT) and were used as controls throughout the study. Mice with a disrupted PPARγ binding site in the *Pck1* promoter were identified as homozygous (PPARE$^{-/-}$) for the mutation. We screened the PPARE$^{-/-}$ mice by polymerase chain reaction (PCR) analysis using primers spanning the PPARE site within the *Pck1* promoter. Primer sequences were as follows: forward primer 5′-AGC CAC TTC TTC TGT ACC-3′ and reverse primer 5′-GTA AGC TTT GTT CTG ACA GG-3′. The *Xho*I restriction endonuclease was used to digest the PCR products and to identify the mutant allele. The mice were housed in microisolator cages and maintained on a 12-h light-dark cycle. Mice had free access to water and were fed a normal mouse diet (LabDiet, St. Louis, MO; Diet #5P76). The approximate composition of the diet was 1.08 kJ protein, 0.58 kJ fat, and 14.33 kJ carbohydrate. The diet consisted of 4100 kJ × kg^{-1} gross energy (16). All experimental protocols were approved by the Case Western Reserve University Institutional Animal Care and Use Committee (IACUC).

Real-time quantitative reverse transcription PCR

Total RNA was prepared from 30 mg of liver with the RNeasy Mini kit (Qiagen, Valencia, CA) and from 100 mg of epididymal WAT and BAT with the RNeasy Lipid Tissue Mini kit (Qiagen, Valencia, CA). We synthesized single-strand cDNA from 2 μg of total RNA with random hexamer primers and MMTV reverse transcriptase (Ambion, Austin, TX) and amplified the cDNAs using the SYBR Green PCR Core reagent mix (Applied Biosystems, Foster City, CA). Real-time quantitative reverse transcription PCR (qRT-PCR) was performed in a Chromo4 Cycler (MJ Research), and the relative amounts of mRNA were determined using a linear regression from the standard curve derivative maximum method using the Opticon Monitor 3 software (MJ Research) as previously described (17). The observed mRNA expression levels were normalized to the 18S rRNA levels. The utilized primer sequences (IDT, Coralville, IA) are presented in supplementary Table I).

Biochemical assays

Male mice were deprived of food overnight, and then heart punctures were performed under anesthesia (tribromoethyl alcohol at 249 mg × kg^{-1}) to collect blood. We generated plasma using Microtainer plasma separator tubes (Becton Dickinson, Franklin Lakes, NJ). Veterinary Diagnostic Services (Marshfield Laboratories, Marshfield, WI) measured the levels of cholesterol, β-hydroxybutyrate, FFA, and triglycerides with an automated analyzer (Roche Modular Autoanalyzer). We assayed the liver triglycerides using the Triglyceride Glycerol Phosphate Oxidase (GPO) reagent as previously described (18) (Pointe Scientific, Lincoln Park, MI). Plasma insulin concentrations were measured with an Ultrasensitive Mouse Insulin ELISA according to the manufacturer's instructions (Mercodia, Winston Salem, NC).

Insulin measurements and glucose tolerance tests

Male mice were deprived of food overnight for 18 h, and 2 g glucose × kg^{-1} of body weight was injected intraperitoneally (IP) into the mice. Blood was collected from the tail vein, and plasma insulin concentrations were measured at 0 and 30 min after glucose injection. Plasma insulin concentrations were measured as described above. Glucose tolerance tests (GTT) were performed on a separate group of male mice. Briefly, we starved the mice (8 weeks old) for 18 h, subsequently injected IP 2 g glucose × kg^{-1} of body weight, collected blood from the tail vein, and measured glucose levels at 0, 15, 30, 60, and 120 min using an UltraTouch Glucose Meter®.

Hyperinsulinemic-euglycemic clamp study

Clamp studies were performed at the Vanderbilt University Mouse Metabolic Phenotyping Core (MMPC) in Nashville, Tennessee. The clamp studies were conducted in WT and PPARE$^{-/-}$ mice at 12–14 weeks of age. The surgical procedures utilized for implanting chronic jugular vein and carotid artery catheters have been previously described (19, 20). Mice were allowed to recover from surgery for ⩾5 days and were studied when body weight was restored to within 10% of the presurgery weight. The clamp was performed in mice fasted for 5 h. A continuous (0.05 μCi × min^{-1}) infusion of HPLC-purified (21) ^{3}H-glucose was initiated 120 min before the clamp. At $t = 0$ min, the basal glucose concentration and specific activity were determined, after which a constant infusion of regular human insulin (2.5 mU × kg^{-1} × min^{-1}) and red blood cells (3 μl/min) was initiated. The ^{3}H-glucose infusion rate was increased (0.1 μCi/min) to minimize changes in glucose specific activity. Glucose (20%) was infused at a variable rate to maintain euglycemia. Glucose levels were tested every 10 min from the carotid artery catheter. At $t = 80$, 90, 100, and 120 min, the plasma glucose specific activity was assessed. At $t = 120$ min, a 12-μCi bolus of 2-deoxyglucose (DG) was administered (22). Blood (30 μl per mouse) was sampled at different times

(t = 122, 125, 130, 135, and 145 min) to determine the arterial blood glucose and plasma DG concentrations (22). We also analyzed the concentrations of plasma FFA and glycerol under clamp conditions using the FFA and free glycerol kits (Zen-Bio Inc., Research Triangle Park, NC) following the manufacturer's directions. At t = 145 min, a blood sample (100 μl) was obtained, and the mice were anesthetized with an infusion of sodium pentobarbital. Tissues (gastrocnemius, superficial vastus lateralis, and soleus muscles, as well as brain, epididymal fat, and liver) were removed, immediately frozen in liquid nitrogen, and stored at −70°C until further analysis. The rate of whole body glucose appearance (R_a) was calculated as the ratio of the ^{3}H-glucose infusion rate (dpm × kg^{-1} × min^{-1}) and plasma glucose specific activity (dpm/mg). The rate of endogenous glucose appearance during the hyperinsulinemic clamp was calculated as the difference between R_a and the exogenous glucose infusion rate. We isolated RNA from the liver (100 mg) and measured *Pck1* expression as described above.

Portal vein injection of insulin

To observe the effects of the PPARE mutation in the *Pck1* promoter on insulin signaling, insulin (1 mU × kg^{-1} body weight) was administered to anesthetize mice by injection into the portal vein. Liver, skeletal muscle, and fat biopsies were removed before (basal) and 5 min after the insulin injection. We snap-froze the tissues for analysis by Western blot analysis.

Islets isolation and insulin secretion

Islets were isolated by the Islet Procurement Core Facility at Vanderbilt University (Nashville, TN) as previously described (23–25). The islets were isolated from WT and PPARE$^{-/-}$ mice by dissection of the splenic portion of the pancreas followed by digestion with collagenase P (Roche Molecular Biochemicals) (26). After a purification procedure, islets were rinsed three times with 12 ml of RPMI-1640 media containing 10% fetal bovine serum, 100 IU/ml penicillin, 100 μg/ml streptomycin, and 5 mM glucose and then cultured in 10-cm untreated plates overnight at 37°C. As islets from WT and PPARE$^{-/-}$ mice varied in diameter, we hand-picked islets under a stereomicroscope and matched them by size. This common microscopic analysis is based on individual islet sizing, calculation of the frequency distribution, and conversion into an islet equivalent (IEQ), which is the volume of a spherical islet with a diameter of 150 mm (27). On the following day, 20 IEQs were incubated in 2 ml of RPMI-1640 media with 5 mM or 16.7 mM glucose. At the end of a static incubation, islets were collected in 1.5-ml tubes and washed three times with 1 ml of 1× PBS, and insulin was extracted in 0.2 ml of acid alcohol for 48 h at 4°C. The media from the static incubation was harvested in 15-ml conical tubes and centrifuged at 2000 rpm. Islet insulin extracts and the static incubation media were stored at −80°C until insulin measurement by radioimmunoassay. The results are expressed as ng of insulin secreted per 100 IEQs for 30 min. The total islet insulin concentration (% content) was calculated as ng of insulin in the media per ng of insulin isolated from the islets at the end of 30 min.

Protein isolation for Western blotting

Proteins were isolated from the liver, kidney, WAT, BAT and skeletal muscle from PPARE$^{-/-}$ and WT mice. A piece of tissue was homogenized in 15 ml/g of tissue of ice-cold homogenizing buffer consisting of 20 mM Tris-HCl, pH 7.6, 0.1 mM EDTA, 0.5 mM EGTA, 1.0% Triton-X, 250 mM sucrose, and 50 μl/5 ml protease inhibitor mixture as described previously (28). The concentration of protein was measured with the Bio-Rad protein assay reagent using BSA as a standard.

Electrophoresis and Western blotting

We sonicated the protein samples for 20 s, and 10–20 μg of protein was diluted in Laemmli sample buffer (100 mM Tris-HCl, pH 6.8, 20% β-mercaptoethanol, 4% SDS, 0.2% bromophenol blue, and 20% glycerol) and separated by 10% SDS-PAGE. For analysis of PCK1, 0.8 mg of liver and kidney proteins and 10 mg of WAT and BAT proteins were loaded. For AKT phosphorylation analysis, 15 μg of liver, WAT, and skeletal proteins were loaded on 10% SDS-PAGE gels. Proteins were electrophoretically transferred to Immobilon® polyvinylidene difluoride membranes, and gels were stained with Coomassie stain (45% methanol, 10% acetic acid, and 2.5% Coomassie Blue R250). The polyvinylidene difluoride membrane was incubated with antibody to PCK1 (1.5 μg/ml) diluted 1:1000 in blocking buffer for 4 h at 22°C, followed by extensive washing with Tris-buffered saline (150 mM NaCl, 10 mM Tris, and 0.05% Tween 20). The primary PCK1 antibody was a generous gift from Richard W. Hanson (Case Western Reserve University). The blots were incubated with 1:10,000 secondary antibody linked to horseradish peroxidase (Santa Cruz Biotechechnology, Inc., Santa Cruz, CA) in 10 ml of blocking buffer for 1 h at 22°C and washed again. Normalization for loading differences was done with an HSC70 antibody diluted at 1:16,000 (Santa Cruz Biotechnology) and anti-mouse IgG-HRP conjugated secondary antibody at 1:10,000 (Santa Cruz Biotechnology). Immunoreactive proteins were detected using the Super-Signal Chemiluminescent Substrate® Kit, and the density of the immunoreactive bands was measured by scanning densitometry using the UN-Scan-IT software (Silk Scientific, Inc., Orem, UT). For portal vein injection of insulin studies, the polyvinylidene difluoride membrane was incubated with antibodies to phosphorylated AKT-Ser^{473}, phosphorylated AKT-Thr^{308}, and total AKT (Cell Signaling Technology, Beverly, MA) diluted in blocking buffer for 4 h at 22°C. The blots were washed and incubated with secondary antibody, and immunoreactive proteins were detected as described above.

Adipocyte lipolysis

Wild-type and PPARE$^{-/-}$ male mice were sacrificed, and epididymal fat pads were removed and weighed. Adipose cells were isolated from gonadal fat pads (2–3 mice per experiment) by collagenase digestion (1 mg/ml, collagenase CLS Type I, Worthington Biochemical Corp., Lakewood, NJ). Cells were incubated at 37°C with constant shaking in Krebs-Ringer-Phosphate (KRP) buffer (50 mM HEPES, pH 7.4, 128 mM NaCl, 4.7 mM KCL, 1.25 mM $CaCl_2$, 1.25 mM $MgSO_4$, 10 mM sodium phosphate and 2.0 mM pyruvic acid) and 2.5% BSA (BSA)-FFA free and in the absence (basal) or presence of insulin (100 nM) or epinephrine (10 μM). Concentrations of FFA released from the adipocytes were measured using a commercial kit (Zen-Bio Inc., Research Triangle Park, NC) following the manufacturer's directions. Total cell protein was prepared from adipocytes using a commercial lysate butter (Promega, Madison, WI). The protein concentration was measured with the Bradford assay (Bio-Rad Protein Assay) using BSA as a standard.

Determination of glycerol kinase activity

GyK activity was measured as previously described (29, 30). Briefly, WAT, BAT, or liver was homogenized in extraction buffer (50 mM HEPES, pH 7.8, 40 mM KCl, 11 mM $MgCl_2$, 1 mM EDTA, and 1 mM DTT) on ice. The samples were centrifuged at 15,000 g for 15 min at 4°C, and 10 μg of protein was used for the enzymatic assay. The protein samples were incubated with 50 μl of assay buffer (50 mM Tris-HCl, pH 7.2, 5 mM ATP, 10 mM $MgCl_2$, 100 mM KCl, 2.5 mM DTT, 4 mM glycerol, and 500 μmol/l ^{3}H-glycerol) for 90 min at 37°C. The reaction was terminated with

100 μl stop solution (ethanol:methanol, 97:3). Equal amounts of samples (20 μl) were spotted onto DE81 Whatman filters (Whatman). The filters were air-dried and washed in water overnight. Radioactivity on the filters was measured by liquid scintillation counting.

Mitochondrial enzyme activity

BAT (20 mg) was homogenized in 1 ml of MSM-EDTA buffer (220 mM mannitol, 70 mM sucrose, 5 mM Mops, and 2 mM EDTA, pH 7.4) supplemented with 1 mg cholate/1 mg wet wt and 1 μl/ml mammalian protease inhibitor cocktail (Sigma-Aldrich, St. Louis, MO) (31). Mitochondrial content was assessed by measuring the succinate dehydrogenase (SCD) and citrate synthase (CS) activities by established spectrophotometric methods (31). Activities were normalized to the tissue wet weight (mg) and protein (μg/μl) and expressed as nmol/min/mg tissue or nmol/min/total protein.

Measurement of ATP concentrations in adipose tissues

In male PPARE$^{-/-}$ and WT mice, ATP tissue concentrations were measured in BAT and WAT. Samples were dissected from mice under anesthesia and flash-frozen. ATP tissue concentrations were analyzed enzymatically from 25–30 mg of tissue as previously described (32) and reported as nmol/mg wet tissue weight.

Measurement of triglyceride concentrations and synthesis by stable isotopes

The Mouse Metabolic Phenotyping Center (MMPC) of Case Western Reserve University (Cleveland, OH) measured the triglyceride content and newly synthesized triglyceride levels. To enrich the body water with ~2% ^{2}H, MMPC administered an IP injection of labeled water (20 μl × g^{-1} of body weight of 9 g/l NaCl in 99% atomic percentage excess ^2H_2O) into adult male mice, and the mice were returned to their cages and maintained on 5% ^{2}H-labeled drinking water for 5 days. The mice were killed, and blood and tissue samples were collected and flash-frozen in liquid nitrogen. The samples were stored at −80°C until analysis. MMPC measured triglyceride concentrations and de novo lipogenesis as previously described (33). Briefly, triglyceride from tissues was isolated, and labeled glycerol and palmitate were analyzed after derivatization by mass spectrometry. The ^{2}H-labeled triglyceride covalently linked to glycerol measures the amount of newly synthesized triglyceride, and the ^{2}H-labeled triglyceride covalently attached to palmitate indicates the amount of new palmitate. In mice given ^2H_2O for 5 days, the contribution of de novo lipogenesis to the pool of triglyceride and palmitate was calculated using the following equation: % newly made palmitate = [total ^{2}H-labeled palmitate × (^{2}H-labeled body water × n)]$^{-1}$ × 100 where n is the number of exchangeable hydrogens, which is assumed to 22 (34, 35). The percentage of total newly made triglyceride glycerol was calculated using the following equation: % total newly made triglyceride-glycerol = [^{2}H-labeled triglyceride-glycerol × (^{2}H-labeled water × n)]$^{-1}$ × 100 where ^{2}H-labeled triglyceride-glycerol is the M1 isotopomer, ^{2}H-labeled water is the average amount labeled in a given mouse, and n is the exchange factor (experimentally determined from the M2/M1 ratio of triglyceride glycerol). We calculated the total triglyceride pool size (μmol/g tissue) in the tissues using the following equation: Total pool size of triglyceride = [^{2}H-labeled triglyceride-glycerol × (^{2}H-labeled water × n)]$^{-1}$ × 100.

Cold exposure of mice

Adult male WT and PPARE$^{-/-}$ mice were cold-challenged by placing individually housed mice into a cold room (4°C) for 4 h. Rectal body temperatures were taken at 0, 1.5, 3, and 4 h. At the conclusion of the study, the mice were killed, and plasma and tissues were collected. We measured plasma FFA and free glycerol as described above. RNA was isolated from BAT, and UCP-1 mRNA expression was measured by qRT-PCR as described above. The utilized primer sequences for UCP-1 (IDT, Coralville, IA) are presented in supplementary Table I.

Measurement of energy expenditure by indirect calorimetry

Metabolic rates were measured by indirect calorimetry in WT and PPARE$^{-/-}$ mice using an 8-chamber, open-circuit Oxymax system (CLAMS, Columbus Instruments, Columbus, OH) at the Mouse Metabolic Phenotyping Center of the University of Cincinnati (Cincinnati, OH). Briefly, mice were individually housed in acrylic calorimeter chambers through which air with a known O_2 concentration was passed at a constant flow rate. The system automatically withdrew gas samples from each chamber hourly for 24 h. The system then calculated the volumes of O_2 consumed (VO_2) and CO_2 generated (VCO_2) by each mouse in 1 h. The RQ, which is the ratio of VCO_2 to VO_2, was calculated. Heat expenditures measured throughout the study measurements were carried out in both light and dark cycles in both fed and fasting conditions and are represented as Kcal/g/day. Mice were maintained at 25°C and had free access to water in all conditions.

Statistical analysis

Results are expressed as the means ± SEM. For analysis of two means, we used the Student t-test. For analysis of 2 × 2 parameters, we used two-way ANOVA with Bonferroni's adjustment. For three comparisons, we analyzed the parameters by one-way ANOVA with Bonferroni's adjustment. The response to GTT was measured by determining the areas under the curve above baseline (AUC) using GraphPad Prism 4. Data that failed Bartlett's test for variance were analyzed with the Kruskal-Wallis test.

RESULTS

PEPCK-C mRNA expression in PPARE$^{-/-}$ mice

We measured *Pck1* mRNA in various tissues from food-deprived WT and PPARE$^{-/-}$ adult male mice by quantitative real-time RT-PCR (**Fig. 1A**). The *Pck1* mRNA levels were decreased in the liver (63% of WT), in WAT (0.2% of WT) and in BAT (6.0% of WT), yet the expression of renal *Pck1* was unaffected. It has previously been shown that *Pck1* mRNA levels reflect the PCK1 protein concentration and enzyme activity (36). To determine if the protein levels were also altered, we analyzed PCK1 by Western blot analysis (Fig. 1B). We found that PCK1 was ablated in WAT and greatly reduced (33% of WT) in BAT. The liver and kidney proteins, however, were equal to WT levels of PCK1.

Effect of altered PEPCK gene expression

To determine the metabolic consequences of altered *Pck1* gene expression in WAT, we measured the fasting levels of glucose, triglycerides, free fatty acids, β-hydroxybutyrate, and cholesterol in the blood as well as triglyceride levels in the livers of fasted male mice (**Table 1**). Male PPARE$^{-/-}$ mice had elevated levels of plasma glucose (13% more than WT), FFA (26% more than WT), β-hydroxybutyrate

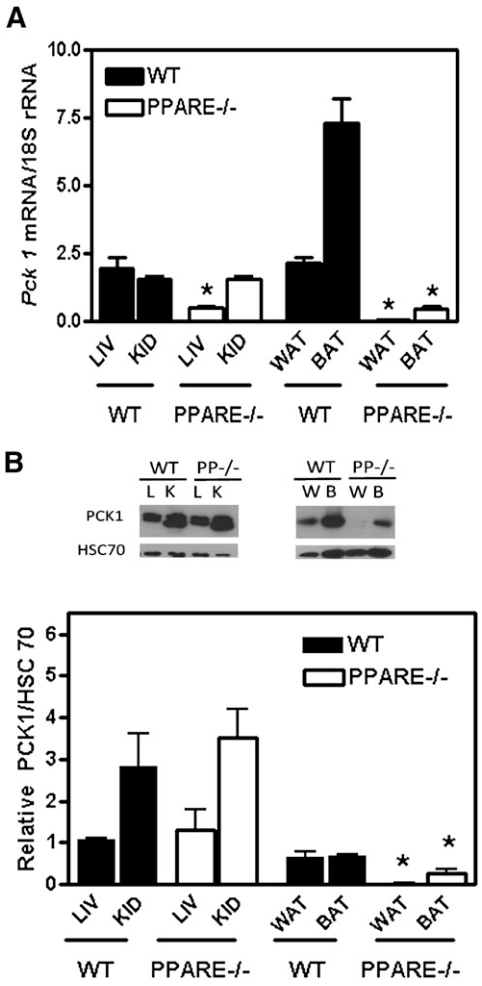

Fig. 1. Expression of Pck1 in liver, kidney, white adipose tissue, and brown adipose tissue. A: Quantitative RT-PCR measurements of *Pck1* mRNA and normalized to 18S rRNA. Values represent the means ± SEM of n = 4–8 mice. *$P < 0.05$ compared with wild-type mice for the same tissue. B: Western Blot analysis of PCK1 in LIV, KID, WAT, and BAT and normalized to HSC-70. Values represent the means ± SEM of n = 4 mice. *$P < 0.05$ compared with wild-type mice for the same tissue. BAT, brown adipose tissue; KID, kidney; LIV, liver; WAT, white adipose tissue; WT, wild type.

(60% more than WT), and cholesterol (25.7% more than WT) and increased hepatic triglycerides (34% more than WT). The PPARE$^{-/-}$ mice had reduced fasting insulin levels (50% less than WT).

PPARE$^{-/-}$ mice exhibit insulin resistance

To establish whether we could observe metabolic differences in the fed state, we analyzed peripheral insulin resistance by GTT (**Fig. 2A**). The means of each time point were compared with WT mice and were significantly different at several time points (*$P < 0.05$). The PPARE$^{-/-}$ mice had reduced glucose clearance as demonstrated by the greater AUC compared with WT mice (25020 ± 1202 and 19460 ± 1309 mg/dl × 120 min for PPARE$^{-/-}$ and WT mice, respectively). The AUCs were significantly different ($P < 0.05$). Reduced glucose clearance may be caused by reduced insulin secretion in response to glucose. Therefore, we measured plasma insulin concentrations in response to a bolus glucose injection in WT and PPARE$^{-/-}$ mice. WT and PPARE$^{-/-}$ mice had similar levels of insulin at 30 min after glucose injection (Fig. 2B); however, at 0 min, the PPARE$^{-/-}$ mice exhibited significantly reduced plasma insulin ($P < 0.05$) (Fig. 2B). This suggests that insulin secretion may be attenuated. To analyze islet function, β-islets were isolated and treated with 5 mM and 16.7 mM glucose. The β-islets from PPARE$^{-/-}$ mice contained and secreted more insulin at 16.7 mM glucose compared with WT mice (Fig. 2C, D).

TABLE 1. Concentrations of blood glucose and plasma metabolites in food-deprived WT and PPARE$^{-/-}$ mice

Males	WT	PPARE$^{-/-}$
Body weight (g)	20.8 ± 0.3	24.2 ± 0.5[a]
Epididymal fat pad (g)	0.2 ± 0.02	0.2 ± 0.03
Glucose (mg/dl)	80.0 ± 2.9	92.5 ± 4.5[a]
Insulin (μg/l)	0.4 ± 04	0.2 ± 0.03[a]
Cholesterol (mg/dl)	77.7 ± 7.4	104.6 ± 9.8[a]
Triglyceride (mg/dl)	40.6 ± 3.6	58.5 ± 10.4
FFA (mM)	0.42 ± 0.03	0.57 ± 0.04[a]
Glycerol (mM)	0.1 ± 0.007	0.1 ± 0.01
β-hydroxybutyrate (mM)	0.6 ± 0.1	1.0 ± 0.1[a]
Triglycerides (mg/g liver)	27.0 ± 3.0	41.1 ± 4.5[a]

Blood measurements are represented as the means ± SEM for 7–15 mice per group. Abbreviations: WT, wild type.
[a] $P < 0.05$ compared with WT male mice.

Peripheral insulin resistance suggests reduced signaling in the AKT pathway. To determine if the insulin-signaling cascade was affected, we administered portal vein injections of insulin (**Fig. 3**). The insulin-signaling pathway was analyzed by phosphorylation of AKT-Ser^{473} and AKT-Thr^{308} and normalized to the total AKT protein. We found that the phosphorylation of AKT-Ser^{473} and AKT-Thr^{308} was greatly reduced in the skeletal muscle and liver (Fig. 3B, C), while phosphorylation of AKT-Thr^{308} was greatly reduced in WAT of PPARE$^{-/-}$ mice (Fig. 3A) ($P < 0.05$).

Reduced glucose uptake in muscle and adipose

To further characterize the insulin resistance, hyperinsulinemic-euglycemic clamp studies were conducted in male PPARE$^{-/-}$ and WT mice. The blood glucose was clamped at 120 mg/dl through glucose administration (**Fig. 4A**), and the glucose infusion rate (GIR) was monitored over 2 h. The PPARE$^{-/-}$ mice exhibited a 40% reduction in GIR on average over the course of the clamp (Fig. 4B). The difference in GIR was evident at 10 min, but it became significantly different at 40 min until the end of the clamp.

The reduced GIR in PPARE$^{-/-}$ mice suggested profound peripheral insulin resistance. The glucose disposal rate was significantly reduced in the PPARE$^{-/-}$ mice (Fig. 4C). Using 2-[^{14}C]deoxyglucose during the clamp, peripheral glucose uptake was measured in the soleus, gastrocnemius, superficial vastus lateralis, WAT, and brain. Glucose uptake was significantly decreased in the soleus, superficial vastus lateralis, and the WAT of PPARE$^{-/-}$ mice (Fig. 4D, E). As a control, glucose uptake was measured in the brain, and it was unaltered.

During the clamp in PPARE$^{-/-}$ mice, insulin suppression of endogenous glucose R_a (endo R_a) was significantly

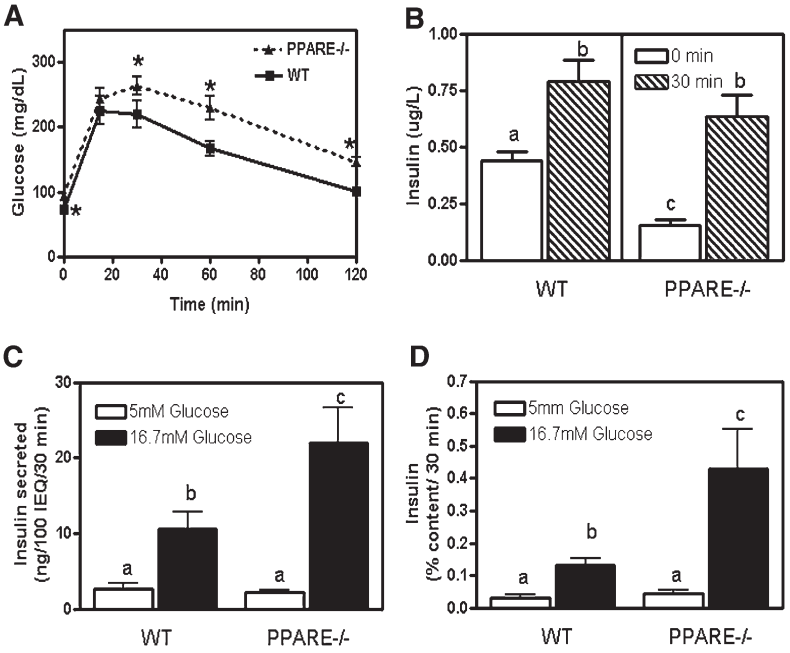

Fig. 2. PPARE$^{-/-}$ mice are insulin resistant. A: Glucose tolerance tests (GTT) in WT and PPARE$^{-/-}$ mice. Values are the means ± SEM of n = 7-10 mice. *$P < 0.05$ compared with WT at that time. B: Plasma insulin concentrations at 0 min and 30 min after glucose injection in male mice. Values are means ± SEM of n = 7–10 mice. Subscripts without a common letter differ, $P < 0.05$. C: Insulin secretion and D: Percentage of insulin concentration from static isolation of WT and PPARE$^{-/-}$ islets. Values are the means ± SEM of n = 5–6 experiments. Subscripts without a common letter differ, $P < 0.05$. BAT, brown adipose tissue; KID, kidney; LIV, liver; WAT, white adipose tissue; WT, wild type.

decreased, suggesting that the infused insulin did not suppress gluconeogenesis (Fig. 4F). We measured the concentration of the *Pck1* mRNA in the liver from mice at the end of the clamp. The levels of *Pck1* were greater in PPARE$^{-/-}$ mice (44% more than WT) even with the insulin infusion during the clamp (**Fig. 5C**). Therefore, PPARE$^{-/-}$ mice exhibited insulin resistance in the liver, muscle, and WAT compared with WT mice.

Lipolysis in PPARE$^{-/-}$ and WT mice

To ascertain the source of the increased fasting FFA, primary adipocytes were isolated from WT and PPARE$^{-/-}$ mice (Fig. 5A). The FFA released in response to insulin (65% more than WT) was greatly increased. Insulin failed to repress the release of FFA in the PPARE$^{-/-}$ mice. We also measured the concentration of glycerol and FFA under clamp conditions. We found that FFA release was greater in PPARE$^{-/-}$ mice (24% more than WT) and glycerol release was greater as well (45% more than WT) (Fig. 5B).

Synthesis of triglyceride in PPARE$^{-/-}$ and WT mice

As mutation of the PPARE region in the promoter of *Pck1* alters its hepatic regulation, we analyzed its effect on triglyceride synthesis as well. Triglyceride and palmitate synthesis rates were measured with the ^2H_2O method (**Fig. 6**). The contribution of de novo lipogenesis to newly synthesized palmitate was equivalent in both genotypes (Fig. 6B). However, the PPARE$^{-/-}$ mice had increased triglyceride synthesis in the liver ($P < 0.05$) and WAT ($P = 0.07$) (Fig. 6A).

Because the amount of glucose uptake in WAT is reduced in PPARE$^{-/-}$ mice during the hyperinsulinemic-euglycemic clamp and PCK1 is ablated, the source of glycerol-3-phosphate for triglyceride must be from another metabolite, such as glycerol. Gyk activity was measured and was higher in WAT of PPARE$^{-/-}$ mice (61% more than WT), yet BAT and liver Gyk were unaltered (Fig. 6C).

Alterations in BAT metabolism

Western blot analysis indicated that PCK1 was lower in BAT of PPARE$^{-/-}$ mice. To determine the metabolic consequences of altered *Pck1* expression, we measured the ATP concentration in BAT (**Table 2**). We found that PPARE$^{-/-}$ mice had 81% less ATP than WT levels. CS and SDH activities were measured and normalized by wet tissue weight (Table 2) and total protein (data not shown), and the activities were equal in WT and PPARE$^{-/-}$ mice. Thus the mitochondrial mass was unchanged, but there may be some perturbations in mitochondrial energetics because ATP levels were so dramatically reduced.

UCP-1 reduces ATP synthesis in BAT, and the resulting energy is lost as heat. To determine if the PPARE$^{-/-}$ mice could tolerate cold exposure, we cold-challenged the mice for 4 h at 4°C. The PPARE$^{-/-}$ mice maintained their body temperature, while WT mice quickly lost body heat. We measured UCP-1 mRNA expression after fasting and cold-challenge and found that PPARE$^{-/-}$ mice had increased levels of UCP-1 after cold-challenge (**Fig. 7B**). Since FFA induces UCP-1 expression, we measured plasma FFA at the end of the cold exposure. The PPARE$^{-/-}$ mice had increased plasma FFA concentrations (27% more than WT) and had less glycerol release under cold-challenge (52% less than WT) (Fig. 7C).

To confirm that the alterations in BAT did not affect overall energy expenditure, we measured energy expenditure by indirect calorimetry over a 24-h period (light and dark cycle) and found relatively minor differences for oxygen consumption in the fed and fasted conditions (supplementary Figs. I and II). Food intakes were also measured and were found to be similar in WT and PPARE$^{-/-}$ mice (4.01 ± 0.14 and 4.2 ± 0.24 g/mouse/24 hr for WT and PPARE$^{-/-}$ mice, respectively; n = 8 mice). The calculated

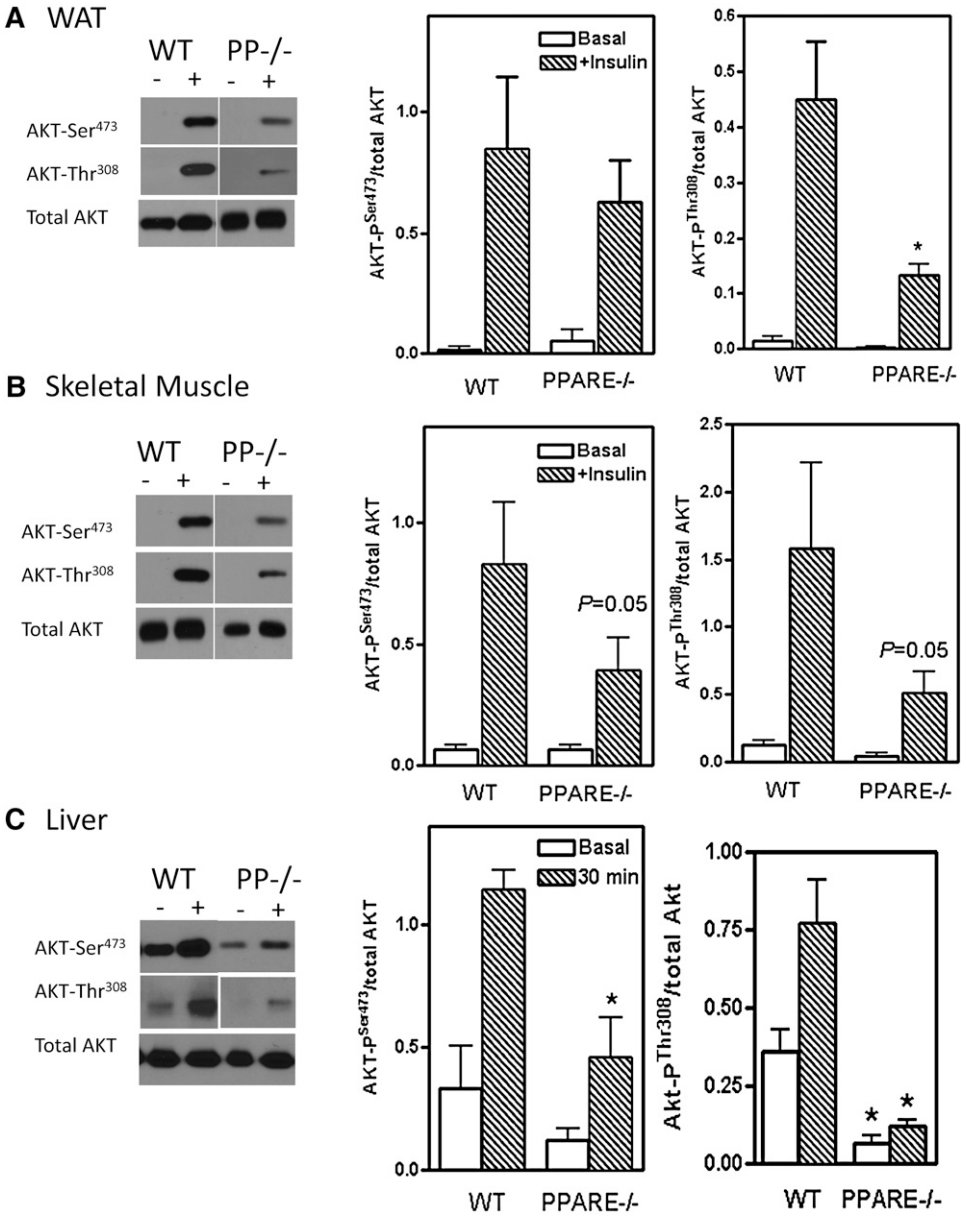

Fig. 3. Reduced AKT phosphorylation in PPARE$^{-/-}$ mice. Western Blot analysis of AKT phosphorylation in (A) WAT, (B) skeletal muscle, and (C) liver before (basal) and after portal vein injection of insulin (+INS) (n = 6 mice per group). The values from the quantified Western blots are shown in the bar graphs. The values are the means ± SEM of n = 3. *$P < 0.05$ compared with WT. WAT, white adipose tissue; WT, wild type.

respiratory quotient was similar in WT and PPARE$^{-/-}$ mice, suggesting similar substrate utilization for energy. However, in the first light cycle, we found a slight decrease in heat production in PPARE$^{-/-}$ mice, which indicates that mitochondrial function might be altered in PPARE$^{-/-}$ mice, but further studies are needed.

DISCUSSION

We hypothesized that the PPARE region of the *Pck1* promoter is essential for the regulation of triglyceride/fatty acid flux between adipose and liver tissues and is important for the maintenance of glucose and lipid homeostasis for the prevention of insulin resistance.

The complex pathogenesis of type 2 diabetes is due to abnormalities that involve insulin action at the peripheral tissues and insulin production in β cells (37). Genetic factors play key roles in the development of type 2 diabetes as well. Beale et al. found two C/T single nucleotide polymorphisms (SNP) in complete linkage disequilibrium at positions -1097 bp and -967 bp of the *Pck1* promoter that are associated with obesity and type-2 diabetes. Patients with T/T polymorphisms have higher HbA1c and higher fasting glucose levels (38). The region of the identified polymorphism in these patients is located within the same PPARE site of the *Pck1* promoter that was deleted in the PPARE$^{-/-}$ mice. Our data in the PPARE$^{-/-}$ mice suggest that dysregulation of *Pck1* in the liver and WAT contributes to the development of insulin resistance.

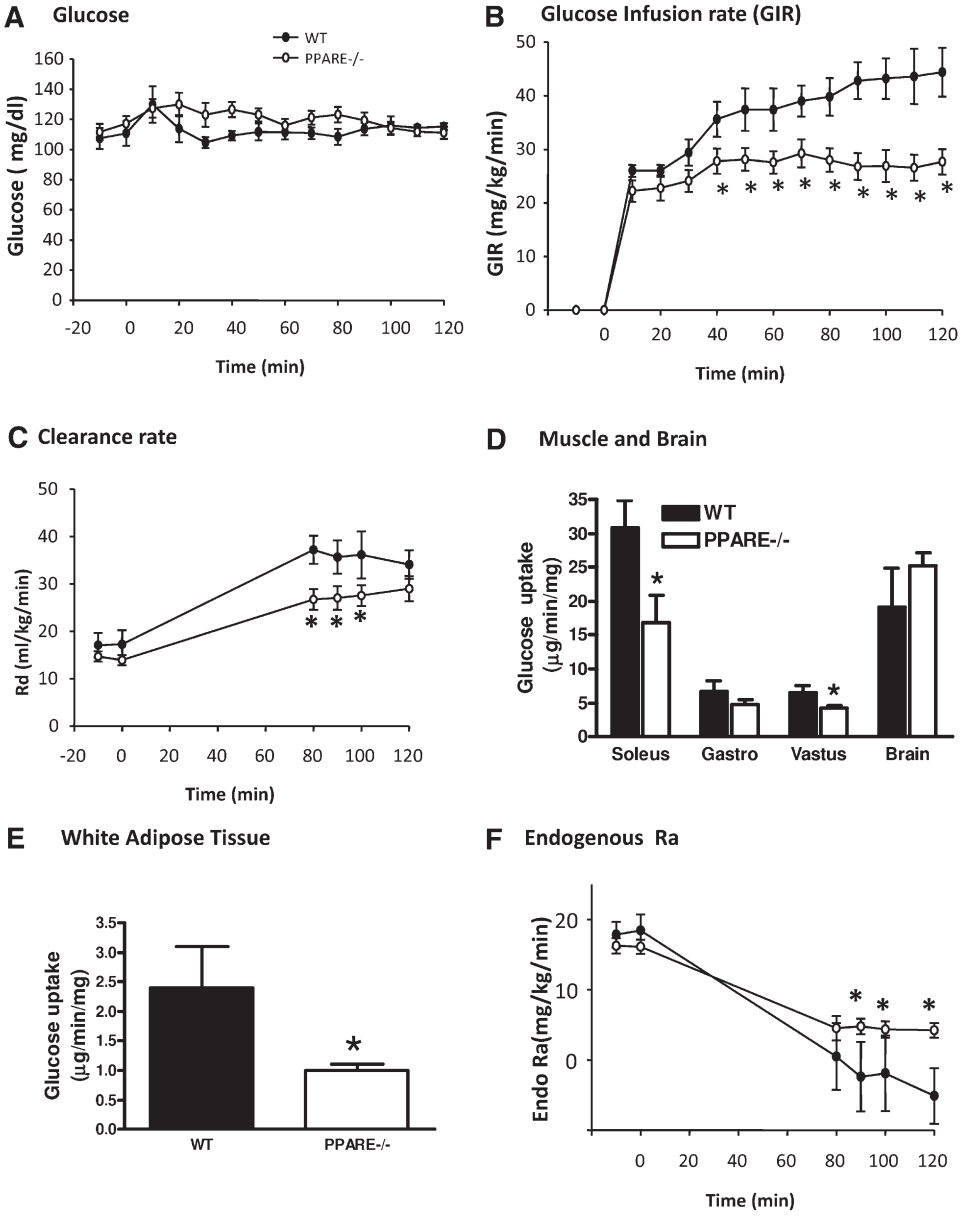

Fig. 4. Hyperinsulinemic-euglycemic clamp in PPARE$^{-/-}$ and WT mice. Glucose clamp was performed in male mice at 12–14 weeks of age. A: Blood glucose levels during the clamp. B: Glucose infusion rate during the course of the clamp. C: Glucose clearance and (D) glucose uptake by skeletal muscles, including soleus, gastrocnemius (Gasto), superficial vastus lateralis (Vastus), and brain. E: Glucose uptake by white adipose tissue (WAT). F: Endogenous glucose appearance rate (R_a) during the clamp. Each data point represents the mean ± SEM of n = 59 mice per group. *$P < 0.05$ compared with WT at that time. WT, wild type.

In adult male PPARE$^{-/-}$ mice, the levels of plasma FFA acids and β-hydroxybutyrate were higher during food deprivation compared with WT mice. This finding was expected as these mice have 2% of the WT level of *Pck1* mRNA in WAT and lack the ability to reesterify FFAs to triglycerides through glyceroneogenesis. The increased FFAs would be oxidized to ketone bodies in the liver. Previously, Olswang et al. established that PPARE$^{-/-}$ mice had a tissue-specific deletion of *Pck1* in WAT only. They found only one out of four PPARE$^{-/-}$ mice had lipodystrophy (15) with mild insulin resistance. However, we found that the PPARE region of the *Pck1* promoter regulates *Pck1* expression in BAT and WAT. After intercrossing (brother × sister mating) for over 20 generations to establish a stable isogenic background, the phenotype of lipodystrophy had been lost. Reshef also reported that backbreeding PPARE$^{-/-}$ mice into the C57Bl/6J background resulted in loss of the lipodystrophy phenotype (unpublished observation). Our data in the current study indicated that ablation of PCK1 in WAT and decreased PCK1 expression in BAT of PPARE$^{-/-}$ mice increased FFA release but did not result in lipodystrophy. This suggests that genetic modifier(s) from the genetic background (B6 × 129/OlaHsd) are required in addition to ablation of Pck1 expression in adipose tissue to produce lipodystrophy. Another example of modifiers resulting in different

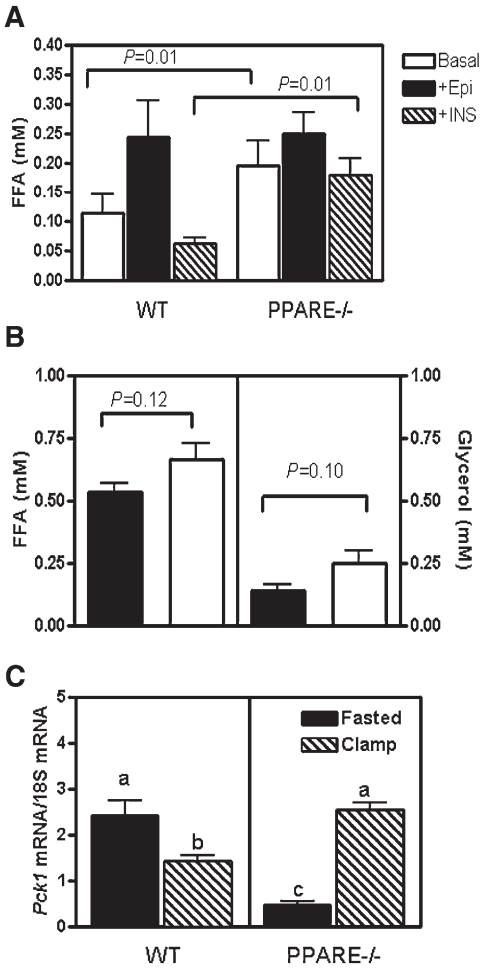

Fig. 5. FFA release from WT and PPARE$^{-/-}$ mice. Measurement of FFA released from (A) isolated adipocytes under basal conditions (time 0) or with insulin (+INS) or epinephrine (+Epi) treatment for 60 min. The values are the mean ± SEM; the subscripts are statistically different from each other at $P < 0.05$. B: Plasma glycerol and FFA concentrations during the hyperinsulinemic-euglycemic clamp. C: Quantitative RT-PCR measurement of *Pck1* mRNA and normalized to 18S rRNA during the hyperinsulinemic-euglycemic clamp. Values are means ± SEM of n = 4 mice. *$P < 0.05$ compared with WT mice for the same tissue. *Pck1,* phosphoenolpyruvate carboxykinase; WT, wild type.

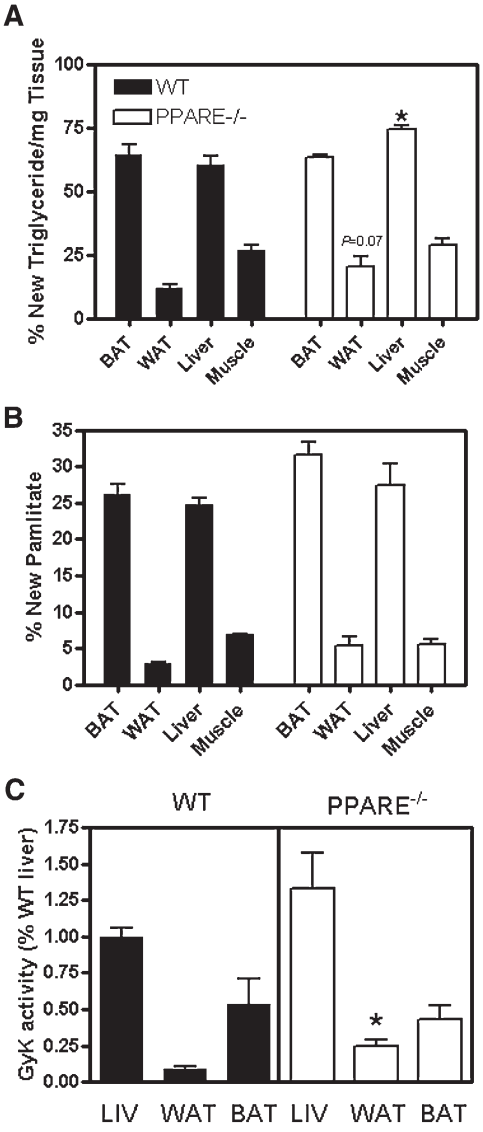

Fig. 6. Triglyceride synthesis and glycerol kinase activity. A: The percent of newly synthesized triglyceride-bound glycerol in isolated tissues after treatment with ^2H_2O for 4 days. B: The percent of newly synthesized triglyceride-bound palmitate in the isolated tissues. Values are presented as means ± SEM of n = 4 per group. *$P < 0.05$ compared with the same tissue in WT mice. C: GyK activity in liver, WAT, and BAT. Values are presented as means ± SEM of n = 4 per group. *$P < 0.05$ compared with the same tissue in WT mice. BAT, brown adipose tissue; GyK, glycerol kinase; WAT, white adipose tissue; WT, wild type.

phenotypic consequences is the varied insulin resistance in the *ir* knockout mice, which encodes for the insulin receptor. Kido et al. have shown that the effect of the *ir* mutation is modified by genetic background (39). In B6 mice, the *ir* null mutation causes mild hyperinsulinemia. In contrast, in 129/Sv mice, the *ir* mutation causes severe hyperinsulinemia (39, 40). Thus mice with different genetic backgrounds can have different metabolic phenotypes as we found in our PPARE$^{-/-}$ in a different background.

The amounts of newly synthesized triglyceride in WAT and liver were higher in PPARE$^{-/-}$ mice (Fig. 6A). This was unexpected since the glycerol-3-phosphate backbone for triglyceride synthesis is usually generated from either glucose (through glycolysis) or lactate and alanine (through glyceroneogenesis). The PPARE$^{-/-}$ mice had reduced glucose uptake in WAT during the hyperinsulinemic-euglycemic clamp and ablated PCK1 expression, so both glycolysis and gluconeogenesis would have attenuated production of glycerol-3-phosphate. However, we found that Gyk activity was significantly increased in WAT of PPARE$^{-/-}$ mice, thus increasing glycerol-3-phosphate synthesis from glycerol stored in lipid droplets. The increased labeling and packaging of VLDL in livers of PPARE$^{-/-}$ mice would also result in increased flux of triglyceride into adipose tissue.

Elevated FFA levels have been shown to cause insulin resistance by impairing insulin signaling through PI(3)K as measured by AKT phosphorylation (41, 42). During the hyperinsulinemic-euglycemic clamp, PPARE$^{-/-}$ mice have increased plasma FFA and glycerol levels, suggesting a lack

TABLE 2. ATP concentration and enzyme activity in WT and PPARE$^{-/-}$ mice

BAT	WT	PPARE$^{-/-}$
ATP concentration (nmol/mg ww)	7.91 ± 2.0	1.58 ± 0.14[a]
CS activity (nmol/min/mg ww)	71.17 ± 2.54	74.52 ± 1.00
SDH activity (nmol/min/mg ww)	0.57 ± 0.3	0.46 ± 0.04

ATP concentration, CS activity, and SDH activity in BAT. Values are the means ± SEM of n = 4. Abbreviations: BAT, brown adipose tissue; CS, citrate synthase; SDH, succinate dehydrogenase, WT, wild type.
[a] $P < 0.05$ compared with WT.

of response to insulin for repression of lipolysis (Fig. 5B). Thus, PPARE$^{-/-}$ mice in both the fed and fasted states have increased plasma FFA concentrations. We found that insulin injections into the portal vein resulted in dramatically reduced hepatic and skeletal muscle AKT-Ser^{473} and AKT-Thr^{308} phosphorylation in PPARE$^{-/-}$ mice; therefore, PPARE$^{-/-}$ mice have reduced insulin signaling in the tissues tested. Cassuto et al. have shown that insulin treatment of isolated hepatocytes resulted in phosphorylation of FOXO1 and disassociation from the AF2, dAF1 (same as PPARE site) and dAF2 sites in the *Pck1* promoter, thus inhibiting *Pck1* expression (43). This suggests that in our study the reduced insulin signaling as well as a loss of the PPARE site contributed to dysregulation of *Pck1* and the triglyceride–fatty acid cycle.

Insulin resistance in the liver also results in an inability to suppress hepatic glucose output. In the hyperinsulinemic-euglycemic clamp, endo R_a is an indicator of glucose output in the liver. We found that suppression of hepatic glucose output by insulin infusion was reduced in the PPARE$^{-/-}$ male mice, indicating hepatic insulin resistance. In the fed state, insulin inhibits gluconeogenesis by suppressing the hepatic transcription of *Pck1* and glucose-6-phosphatase (44). The PPARE$^{-/-}$ mice have increased hepatic *Pck1* expression in response to the hyperinsulinemic-euglycemic clamp (Fig. 5C). This suggests that hepatic insulin regulation may require the PPARE region of the *Pck1* promoter or that hepatic *Pck1* regulation may be secondary to alterations in adipose tissue.

Alterations in BAT metabolism may also contribute to insulin resistance. In PPARE$^{-/-}$ mice, the BAT had greatly reduced expression of *Pck1* mRNA and protein. It has been established that BAT has significant glyceroneogenesis activity, which regulates the rate of reesterification of fatty acids. Reduced reesterification of FFAs should increase UCP-1 expression (11, 45); however, we did not find a dramatic increase in UCP-1 in the fasted state for PPARE$^{-/-}$ mice. One possible explanation is that BAT has significant Gyk activity, and the PPARE$^{-/-}$ mice may depend more on GyK activity for the generation of glycerol-3-phosphate to maintain triglyceride stores. We found that the food-deprived PPARE$^{-/-}$ mice had a decreased ATP concentration in BAT despite having similar mitochondrial mass. Burgess et al. analyzed PCK flux and regulation of energy metabolism and gluconeogenesis by NMR analysis (46). They suggested that PCK1 flux correlates with energy generated in the TCA cycle. In mice with ablated hepatic PCK1, ATP levels were greatly reduced. Although

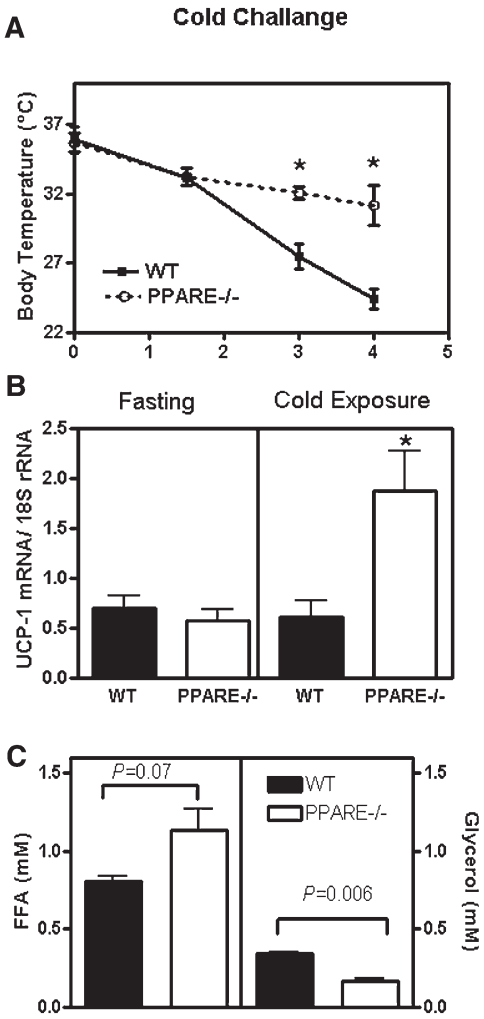

Fig. 7. Increased body temperature and UCP-1 mRNA expression in PPARE$^{-/-}$ mice. A: The body temperatures of WT and PPARE$^{-/-}$ mice during cold challenge at 4°C. Values are means ± SEM of n = 4. *$P < 0.05$ compared with WT at that time. B: Quantitative RT-PCR analysis of UCP-1 mRNA expression in BAT. The values are the mean ± SEM of n = 4 mice per group. *$P < 0.05$. C: Plasma glycerol and FFAs concentrations at the end of the cold challenge. The values are means ± SEM of n = 3 mice per group. *$P < 0.05$. BAT, brown adipose tissue; UCP, uncoupling protein; WT, wild type.

their data was focused on the liver, this may explain the reduced ATP generation in BAT of fasted PPARE$^{-/-}$ mice. The indirect calorimetry data suggested moderate alterations in overall energy expenditures, which support that mitochondrial function may be altered in PPARE$^{-/-}$ mice. However, during cold exposure, the PPARE$^{-/-}$ mice maintained their body temperatures for 4 h, while WT mice had a dramatic drop in body temperature. Since glyceroneogenesis is compromised in the PPARE$^{-/-}$ mice, they had increased plasma FFA release from WAT during the stress of cold exposure, which in turn induced UCP-1 expression in BAT to generate nonshivering thermogenesis. The increase in UCP-1 in PPARE$^{-/-}$ mice would increase fatty acid oxidation and generate heat production in mitochondria to maintain the body temperature. More experiments are needed to determine if the PPARE$^{-/-}$ mice

have altered mitochondrial function, which will be the focus of future study.

Finally, we analyzed the consequence of alterations in the triglyceride/fatty acid cycle on insulin secretion from islets. We found that, in the isolated β-islets from PPARE$^{-/-}$ mice, there was a 2-fold increase in insulin secretion at 16.7 mM glucose compared with WT mice. However, PPARE$^{-/-}$ mice had reduced insulin levels after fasting, but 30 min after IP glucose injection there were no differences in plasma insulin levels between PPARE$^{-/-}$ and WT mice. One possible explanation for this discrepancy is that isolation of islets from the pancreas severs the connections between the islet vasculature and the systemic circulation (47). In addition, as the isolated islets measure synthesis of insulin and insulin secretion while whole-body measurements of insulin assess the overall flux of insulin (synthesis, secretion, and degradation), it may be that PPARE$^{-/-}$ mice have increased clearance of insulin. Insulin clearance includes both first-pass hepatic and peripheral insulin uptake and degradation in all insulin-sensitive tissues (48). However, hepatic uptake is influenced by both physiological and pathophysiological factors that are not completely understood (49, 50). This process involves binding to a specific membrane receptor, internalization, intracellular compartmentalization of insulin-receptor complex, and proteolytic degradation by insulin degradation enzyme (IDE) (48). Further studies are needed to fully understand the mechanism of reduced fasting insulin in PPARE$^{-/-}$ mice.

Clearly the PPARE$^{-/-}$ islets have adapted to the insulin resistance. Several potential mediators have been suggested to be signals for the β cells to respond to insulin resistance. These include glucose, FFA, autonomic nerves, fat-derived hormones, and the glut hormone glucagon-like peptide-1 (GLP-1). FFAs have been shown to augment glucose-stimulated insulin secretion in perfused rat pancreas (51). Since we found elevated FFAs in PPARE$^{-/-}$ mice, it is possible that FFAs may be involved in the adaptation of insulin secretion to insulin resistance. Thus, regulation of the triglyceride–FFA cycle may also be critical for maintaining insulin sensitivity in the islets.

CONCLUSION

We have shown that the PPARE region of *Pck1* contributes to the regulation of the triglyceride–FFA cycle in WAT and liver. The PPARE region of the *Pck1* promoter is required for adipose tissue expression of *Pck1*. Ablation of *Pck1* in WAT and reduced expression of *Pck1* in BAT resulted in increased plasma FFA, thus contributing to the development of insulin resistance. In addition, hepatic insulin resistance may be a result of alterations in WAT that cause insulin resistance, or it may be caused by altered regulation of hepatic *Pck1* due to the mutated PPARE region of the *Pck1* promoter. Further studies are required to fully characterize these mechanisms. Therefore, investigation of *Pck1* expression and its regulation in the triglyceride/fatty acid cycle is necessary for our understanding of maintenance of glucose and lipid homeostasis and disease prevention.

The authors thank Dr. Marcela Brissova and Ms. Anastasia Golovin at the Vanderbilt University Islet Procurement and Analysis Core for performing the islet isolation and assessment of islet insulin secretion. The authors thank Ms. Wanda Snead and Mr. Wendell Nicholson at the Vanderbilt University Hormone Assay Core for performing the insulin assay. Both core facilities are supported by the Vanderbilt Diabetes Research and Training Center (P60 DK020593). The PPARE$^{-/-}$ mice were a generous gift from Lea Reshef and Richard W. Hanson.

REFERENCES

1. Pinhas-Hamiel, O., L. M. Dolan, S. R. Daniels, D. Standiford, P. R. Khoury, and P. Zeitler. 1996. Increased incidence of non-insulin-dependent diabetes mellitus among adolescents. *J. Pediatr.* **128:** 608–615.
2. Wild, S., G. Roglic, A. Green, R. Sicree, and H. King. 2004. Global prevalence of diabetes: estimates for the year 2000 and projections for 2030. *Diabetes Care.* **27:** 1047–1053.
3. Randle, P. J. 1998. Regulatory interactions between lipids and carbohydrates: the glucose fatty acid cycle after 35 years. *Diabetes Metab. Rev.* **14:** 263–283.
4. Boden, G. 1997. Role of fatty acids in the pathogenesis of insulin resistance and NIDDM. *Diabetes.* **46:** 3–10.
5. Boden, G. 1998. Free fatty acids (FFA), a link between obesity and insulin resistance. *Front. Biosci.* **3:** d169–d175.
6. Reshef, L., R. W. Hanson, and F. J. Ballard. 1970. A possible physiological role for glyceroneogenesis in rat adipose tissue. *J. Biol. Chem.* **245:** 5979–5984.
7. Ballard, F. J., R. W. Hanson, and G. A. Leveille. 1967. Phosphoenolpyruvate carboxykinase and the synthesis of glyceride-glycerol from pyruvate in adipose tissue. *J. Biol. Chem.* **242:** 2746–2750.
8. Reshef, L., J. Niv, and B. Shapiro. 1967. Effect of propionate on lipogenesis in adipose tissue. *J. Lipid Res.* **8:** 682–687.
9. Hahn, P., and M. Novak. 1975. Development of brown and white adipose tissue. *J. Lipid Res.* **16:** 79–91.
10. Botion, L. M., M. N. Brito, N. A. Brito, S. R. Brito, I. C. Kettelhut, and R. H. Migliorini. 1998. Glucose contribution to in vivo synthesis of glyceride-glycerol and fatty acids in rats adapted to a high-protein, carbohydrate-free diet. *Metabolism.* **47:** 1217–1221.
11. Festuccia, W. T., N. H. Kawashita, M. A. Garofalo, M. A. Moura, S. R. Brito, I. C. Kettelhut, and R. H. Migliorini. 2003. Control of glyceroneogenic activity in rat brown adipose tissue. *Am. J. Physiol. Regul. Integr. Comp. Physiol.* **285:** R177–R182.
12. Kalhan, S. C., S. Mahajan, E. Burkett, L. Reshef, and R. W. Hanson. 2001. Glyceroneogenesis and the source of glycerol for hepatic triacylglycerol synthesis in humans. *J. Biol. Chem.* **276:** 12928–12931.
13. Hanson, R. W., and L. Reshef. 2003. Glyceroneogenesis revisited. *Biochimie.* **85:** 1199–1205.
14. Jensen, M. D., K. Ekberg, and B. R. Landau. 2001. Lipid metabolism during fasting. *Am. J. Physiol. Endocrinol. Metab.* **281:** E789–E793.
15. Olswang, Y., H. Cohen, O. Papo, H. Cassuto, C. M. Croniger, P. Hakimi, S. M. Tilghman, R. W. Hanson, and L. Reshef. 2002. A mutation in the peroxisome proliferator-activated receptor gamma-binding site in the gene for the cytosolic form of phosphoenolpyruvate carboxykinase reduces adipose tissue size and fat content in mice. *Proc. Natl. Acad. Sci. USA.* **99:** 625–630.
16. Mardones, P., P. Strobel, S. Miranda, F. Leighton, V. Quinones, L. Amigo, J. Rozowski, M. Krieger, and A. Rigotti. 2002. Alpha-tocopherol metabolism is abnormal in scavenger receptor class B type I (SR-BI)-deficient mice. *J. Nutr.* **132:** 443–449.
17. Millward, C. A., J. D. Heaney, D. S. Sinasac, E. C. Chu, I. R. Bederman, D. A. Gilge, S. F. Previs, and C. M. Croniger. 2007. Mice with a deletion in the gene for CCAAT/enhancer-binding protein beta are protected against diet-induced obesity. *Diabetes.* **56:** 161–167.
18. Millward, C. A., L. C. Burrage, H. Shao, D. S. Sinasac, J. H. Kawasoe, A. E. Hill-Baskin, S. R. Ernest, A. Gornicka, C. W. Hsieh, S. Pisano, et al. 2009. Genetic factors for resistance to diet-induced obesity and associated metabolic traits on mouse chromosome 17. *Mamm. Genome.* **20:** 71–82.

19. Halseth, A. E., D. P. Bracy, and D. H. Wasserman. 1999. Overexpression of hexokinase II increases insulinand exercise-stimulated muscle glucose uptake in vivo. *Am. J. Physiol.* **276:** E70–E77.
20. Niswender, K. D., M. Shiota, C. Postic, A. D. Cherrington, and M. A. Magnuson. 1997. Effects of increased glucokinase gene copy number on glucose homeostasis and hepatic glucose metabolism. *J. Biol. Chem.* **272:** 22570–22575.
21. Balak, K. J., R. H. Keith, and M. R. Felder. 1982. Genetic and developmental regulation of mouse liver alcohol dehydrogenase. *J. Biol. Chem.* **257:** 15000–15007.
22. Bagby, G. J., C. H. Lang, N. Skrepnik, and J. J. Spitzer. 1992. Attenuation of glucose metabolic changes resulting from TNF-alpha administration by adrenergic blockade. *Am. J. Physiol.* **262:** R628–R635.
23. Brissova, M., M. Blaha, C. Spear, W. Nicholson, A. Radhika, M. Shiota, M. J. Charron, C. V. Wright, and A. C. Powers. 2005. Reduced PDX-1 expression impairs islet response to insulin resistance and worsens glucose homeostasis. *Am. J. Physiol. Endocrinol. Metab.* **288:** E707–E714.
24. Brissova, M., W. E. Nicholson, M. Shiota, and A. C. Powers. 2003. Assessment of insulin secretion in the mouse. *Methods Mol. Med.* **83:** 23–45.
25. Brissova, M., M. Fowler, P. Wiebe, A. Shostak, M. Shiota, A. Radhika, P. C. Lin, M. Gannon, and A. C. Powers. 2004. Intraislet endothelial cells contribute to revascularization of transplanted pancreatic islets. *Diabetes.* **53:** 1318–1325.
26. Stefan, Y., P. Meda, M. Neufeld, and L. Orci. 1987. Stimulation of insulin secretion reveals heterogeneity of pancreatic B cells in vivo. *J. Clin. Invest.* **80:** 175–183.
27. Lembert, N., J. Wesche, P. Petersen, M. Doser, H. D. Becker, and H. P. Ammon. 2003. Areal density measurement is a convenient method for the determination of porcine islet equivalents without counting and sizing individual islets. *Cell Transplant.* **12:** 33–41.
28. Croniger, C. M., C. Millward, J. Yang, Y. Kawai, I. J. Arinze, S. Liu, M. Harada-Shiba, K. Chakravarty, J. E. Friedman, V. Poli, et al. 2001. Mice with a deletion in the gene for CCAAT/enhancer-binding protein beta have an attenuated response to cAMP and impaired carbohydrate metabolism. *J. Biol. Chem.* **276:** 629–638.
29. Hibuse, T., N. Maeda, T. Funahashi, K. Yamamoto, A. Nagasawa, W. Mizunoya, K. Kishida, K. Inoue, H. Kuriyama, T. Nakamura, et al. 2005. Aquaporin 7 deficiency is associated with development of obesity through activation of adipose glycerol kinase. *Proc. Natl. Acad. Sci. USA.* **102:** 10993–10998.
30. Guan, H. P., Y. Li, M. V. Jensen, C. B. Newgard, C. M. Steppan, and M. A. Lazar. 2002. A futile metabolic cycle activated in adipocytes by antidiabetic agents. *Nat. Med.* **8:** 1122–1128.
31. Krahenbuhl, S., M. Chang, E. P. Brass, and C. L. Hoppel. 1991. Decreased activities of ubiquinol:ferricytochrome c oxidoreductase (complex III) and ferrocytochrome c:oxygen oxidoreductase (complex IV) in liver mitochondria from rats with hydroxycobalamin[c-lactam]-induced methylmalonic aciduria. *J. Biol. Chem.* **266:** 20998–21003.
32. Puchowicz, M. A., K. Xu, D. Magness, C. Miller, W. D. Lust, T. S. Kern, and J. C. LaManna. 2004. Comparison of glucose influx and blood flow in retina and brain of diabetic rats. *J. Cereb. Blood Flow Metab.* **24:** 449–457.
33. Bederman, I. R., S. Foy, V. Chandramouli, J. C. Alexander, and S. F. Previs. 2009. Triglyceride synthesis in epididymal adipose tissue: contribution of glucose and non-glucose carbon sources. *J. Biol. Chem.* **284:** 6101–6108.
34. Lee, W. N., S. Bassilian, Z. Guo, D. Schoeller, J. Edmond, E. A. Bergner, and L. O. Byerley. 1994. Measurement of fractional lipid synthesis using deuterated water (2H2O) and mass isotopomer analysis. *Am. J. Physiol.* **266:** E372–E383.
35. Diraison, F., C. Pachiaudi, and M. Beylot. 1997. Measuring lipogenesis and cholesterol synthesis in humans with deuterated water: use of simple gas chromatographic/mass spectrometric techniques. *J. Mass Spectrom.* **32:** 81–86.
36. Chakravarty, K., and R. W. Hanson. 2007. Insulin regulation of phosphoenolpyruvate carboxykinase-c gene transcription: the role of sterol regulatory element-binding protein 1c. *Nutr. Rev.* **65:** S47–S56.
37. Kahn, C. R. 1994. Banting Lecture. Insulin action, diabetogenes, and the cause of type II diabetes. *Diabetes.* **43:** 1066–1084.
38. Beale, E. G., B. J. Harvey, and C. Forest. 2007. PCK1 and PCK2 as candidate diabetes and obesity genes. *Cell Biochem. Biophys.* **48:** 89–95.
39. Kido, Y., N. Philippe, A. A. Schaffer, and D. Accili. 2000. Genetic modifiers of the insulin resistance phenotype in mice. *Diabetes.* **49:** 589–596.
40. Accili, D., Y. Kido, J. Nakae, D. Lauro, and B. C. Park. 2001. Genetics of type 2 diabetes: insight from targeted mouse mutants. *Curr. Mol. Med.* **1:** 9–23.
41. Griffin, M. E., M. J. Marcucci, G. W. Cline, K. Bell, N. Barucci, D. Lee, L. J. Goodyear, E. W. Kraegen, M. F. White, and G. I. Shulman. 1999. Free fatty acid-induced insulin resistance is associated with activation of protein kinase C theta and alterations in the insulin signaling cascade. *Diabetes.* **48:** 1270–1274.
42. Dresner, A., D. Laurent, M. Marcucci, M. E. Griffin, S. Dufour, G. W. Cline, L. A. Slezak, D. K. Andersen, R. S. Hundal, D. L. Rothman, et al. 1999. Effects of free fatty acids on glucose transport and IRS-1-associated phosphatidylinositol 3-kinase activity. *J. Clin. Invest.* **103:** 253–259.
43. Hanson, R. W., and L. Reshef. 1997. Regulation of phosphoenolpyruvate carboxykinase (GTP) gene expression. *Annu. Rev. Biochem.* **66:** 581–611.
44. Cao, W., Q. F. Collins, T. C. Becker, J. Robidoux, E. G. Lupo, Jr., Y. Xiong, K. W. Daniel, L. Floering, and S. Collins. 2005. p38 Mitogen-activated protein kinase plays a stimulatory role in hepatic gluconeogenesis. *J. Biol. Chem.* **280:** 42731–42737.
45. Brito, M. N., N. A. Brito, S. R. Brito, M. A. Moura, N. H. Kawashita, I. C. Kettelhut, and R. H. Migliorini. 1999. Brown adipose tissue triacylglycerol synthesis in rats adapted to a high-protein, carbohydrate-free diet. *Am. J. Physiol.* **276:** R1003–R1009.
46. Burgess, S. C., T. He, Z. Yan, J. Lindner, A. D. Sherry, C. R. Malloy, J. D. Browning, and M. A. Magnuson. 2007. Cytosolic phosphoenolpyruvate carboxykinase does not solely control the rate of hepatic gluconeogenesis in the intact mouse liver. *Cell Metab.* **5:** 313–320.
47. Brissova, M., and A. C. Powers. 2008. Revascularization of transplanted islets: can it be improved? *Diabetes.* **57:** 2269–2271.
48. Castillo, M. J., A. J. Scheen, M. R. Letiexhe, and P. J. Lefebvre. 1994. How to measure insulin clearance. *Diabetes Metab. Rev.* **10:** 119–150.
49. Duckworth, W. C., F. G. Hamel, and D. E. Peavy. 1988. Hepatic metabolism of insulin. *Am. J. Med.* **85:** 71–76.
50. Sato, H., T. Terasaki, H. Mizuguchi, K. Okumura, and A. Tsuji. 1991. Receptor-recycling model of clearance and distribution of insulin in the perfused mouse liver. *Diabetologia.* **34:** 613–621.
51. Stein, D. T., B. E. Stevenson, M. W. Chester, M. Basit, M. B. Daniels, S. D. Turley, and J. D. McGarry. 1997. The insulinotropic potency of fatty acids is influenced profoundly by their chain length and degree of saturation. *J. Clin. Invest.* **100:** 398–403.